



# A cause of natural arm-swing in bipedal walking

Yuichiro Toda<sup>1</sup> · Ying Wang<sup>1</sup> · Mamoru Minami<sup>1</sup>

Received: 23 March 2020 / Accepted: 27 August 2020 / Published online: 17 September 2020  
© International Society of Artificial Life and Robotics (ISAROB) 2020

## Abstract

The research of humanoid is widely discussed whether by simulations or real machines. In human bipedal walking, swinging arms in opposite directions is a natural movement. In this research, a model of the humanoid robot, including slipping, bumping, surface-contacting and point-contacting of the foot has been established, and its dynamical equation is derived by the Newton–Euler method. And the natural arm-swing simulation has been produced, which showed that the input torque in yaw rotation of the torso could cause natural arm-swing. “Natural” means that the arm-swinging motion is induced by coupling effects existing in nonlinear dynamics of humanoid robot even though no torques have been input into shoulders. Based on the results, a hypothesis that the vibration in the yaw rotation of the torso caused natural arm swing is proposed. In this paper, we compared the arm-swing movement with or without the input torque of yaw rotation of the torso by using the above humanoid robot model. The simulation data proved the hypothesis to be valid.

**Keywords** Humanoid · Arm swing · Bipedal walking · Dynamical · Newton–Euler Method

## 1 Introduction

Human beings are deemed to acquired the ability of stable bipedal walking in evolving repetitions so far. Our research has begun from the viewpoint of aiming to describe gait’s dynamics as correctly as possible, including point contacting state of foot, toe slipping of the foot and bumping [1, 2]. Based on [3], the dynamics of humanoid can be modelled as a serial-link manipulator, including constraint motion and slipping motion using the Extended Newton-Euler (NE) Method [4]. The NE method enables us to make a dynamical model of robots by repetitive calculation that is different from Lagrange method. And it is possible to calculate internal force and torque not generating real motion. It seems to be an advantage of the NE method that other methods do not have [5]. This merit can be applicable for propagations of constraint and impact force/torque when discussing humanoids walking based on strict dynamical models.

In previous researches, a walking model of the humanoid robot, including slipping, bumping, surface contacting and point-contacting of the foot were discussed, having paved the way for original strategy of “Visual Lifting Approach” (VLA) [6–8] for generating continuous walking gaits. Since our discussions concerning humanoid’s walking have been based on simulations, we have to be careful for preciseness of the dynamical model used for simulations. So the authors have made efforts to confirm that the used dynamical model represents the humanoid’s motion correctly [9–12]. And the current research about natural arm-swing has been conducted above the basement of the previous researches.

In this research, we focused on human’s natural arm-swinging motions during the walking. Arm swing in human bipedal walking is a natural motion wherein each arm swing with the same phase of the opposite side leg without any input torque in the shoulders and arms. Studies on the role of arm swing consist mainly of analysis of bipedal walking models and treadmill experiments on human subjects [15, 16]. Bipedal walking models of various complexity levels explained the effects of arm swing on human locomotion [17, 18]. However as far as the authors know, no report has clarified the causality of natural arm-swing based on dynamical model with changing constraint conditions of foot contacting.

---

This work was presented in part at the 25th International Symposium on Artificial Life and Robotics (Beppu, Oita, January 22–24, 2020).

---

✉ Yuichiro Toda  
ytoda@okayama-u.ac.jp

<sup>1</sup> 3-1-1 Tsushima-naka, Kita-ku, Okayama, Japan

In this paper, we used the physical humanoid model composed of 17-link and 18 joints that has been built [9–12]. We found that when there was no input in the shoulders joints and the torso in bipedal walking, the arm-swing spontaneously with a same phase in the same direction. While when the torque to yaw rotation of the torso is added, the symmetrical arm-swing appeared with opposite phase. We have examined the causality of how the yaw rotation of torso influences arm-swing through the dynamic coupling by Newton-Euler(NE) Method.

## 2 Dynamical walking model

### 2.1 Humanoid model

In previous researches [1–9], a walking model of the humanoid robot, including slipping, bumping, surface contacting and point-contacting of the foot discussed. Its structure of humanoid model is depicted in Fig. 1. Table 1 lists length  $l_i$  [m], mass  $m_i$  [kg] of links and coefficient of joints' viscous friction  $d_i$  [N·m·s/rad], which are decided based on [13]. The equation of motion is derived by NE formulation according to [19] as:

**Table 1** Physical parameters

Link	$l_i$	$m_i$	$d_i$
Head	0.24	4.5	0.5
Upper body	0.41	21.5	10.0
Middle body	0.1	2.0	10.0
Lower body	0.1	2.0	10.0
Upper arm	0.31	2.3	0.03
Lower arm	0.24	1.4	1.0
Hand	0.18	0.4	2.0
Waist	0.27	2.0	10.0
Upper leg	0.38	7.3	10.0
Lower leg	0.40	3.4	10.0
Foot	0.07	1.3	10.0
Total weight [kg]	–	64.2	–
Total height [m]	1.7	–	–

$$M(q)\ddot{q} + h(q, \dot{q}) + g(q) + D\dot{q} = \tau \tag{1}$$

Here,  $\tau = [f_0, \tau_1, \tau_2, \dots, \tau_{17}]$  is input torque and force,  $M(q)$  is inertia matrix, both of  $h(q, \dot{q})$  and  $g(q)$  are vectors that indicate Coriolis force, centrifugal force and gravity.  $D = \text{diag}[\mu_0, d_1, d_2, \dots, d_{17}]$  is a diagonal matrix which means friction coefficients between foot and ground, and

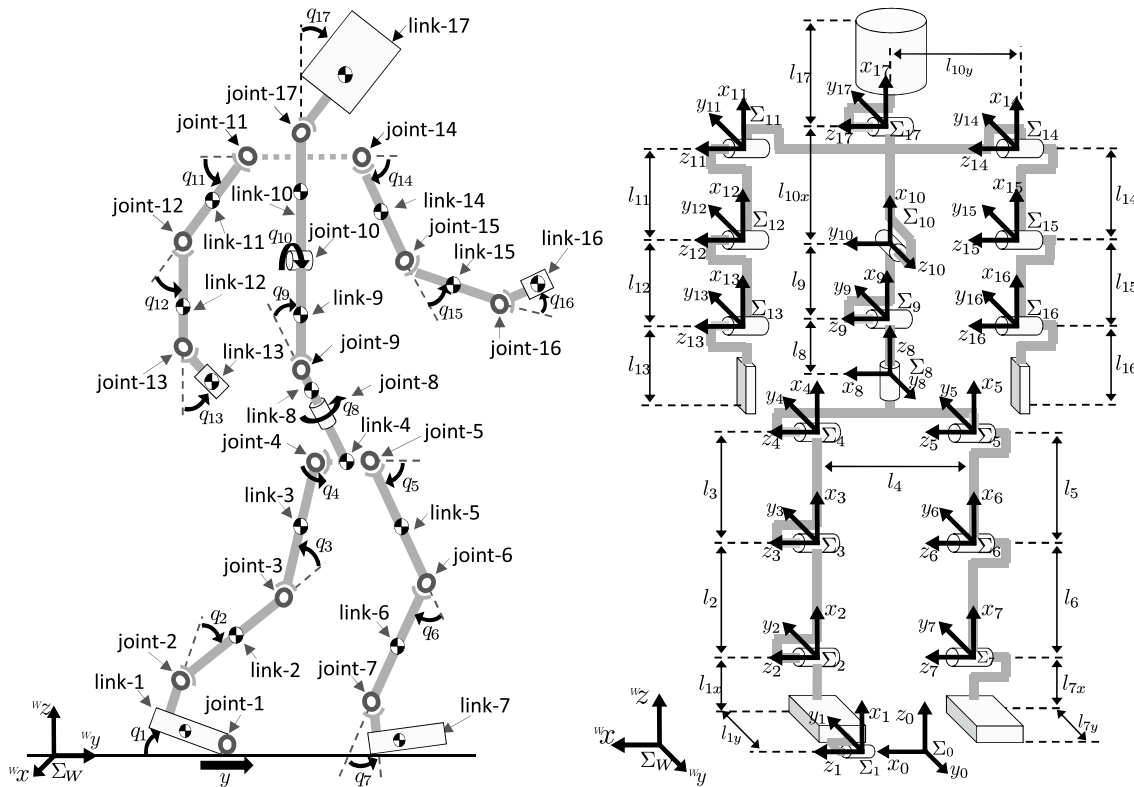
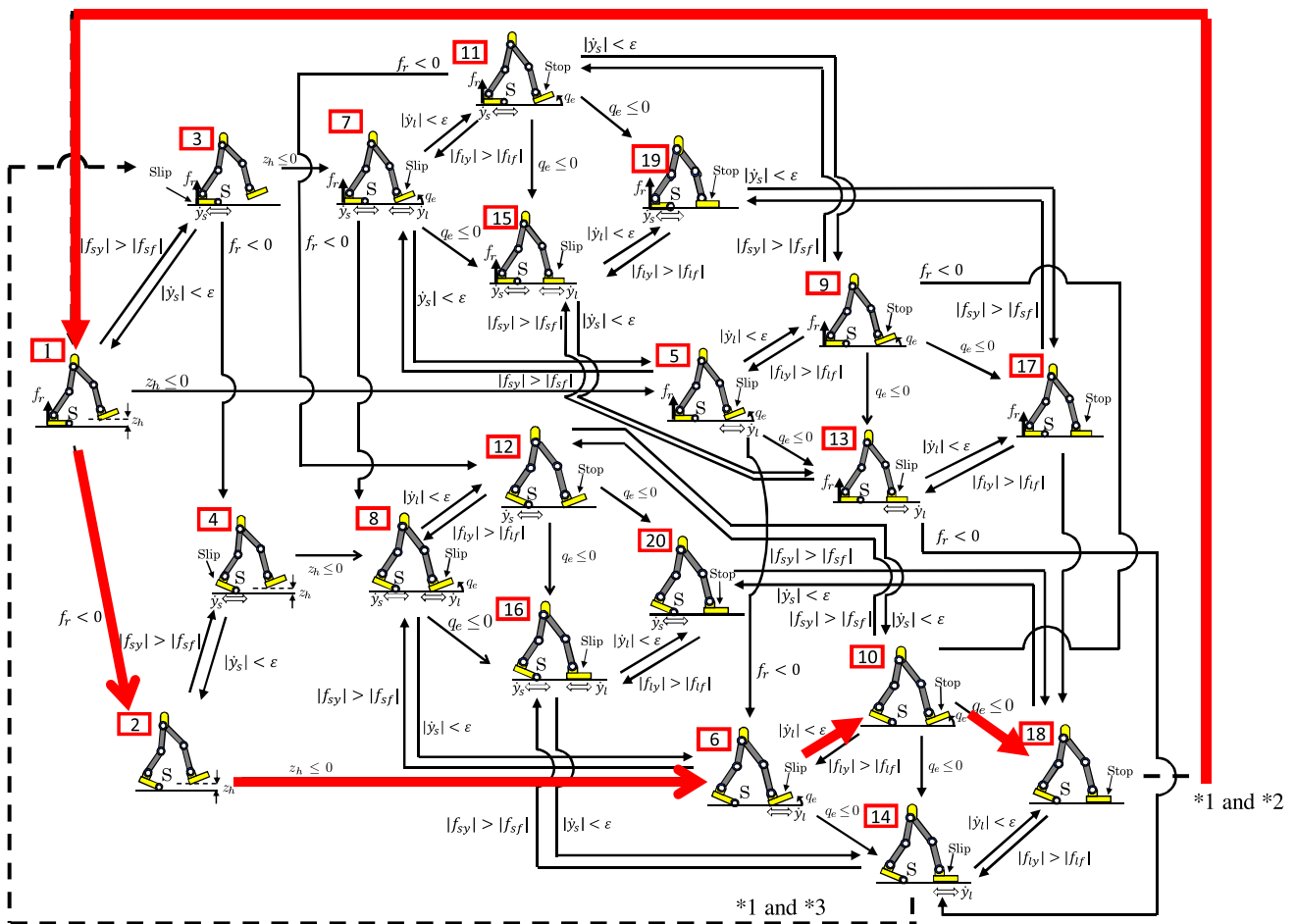


**Fig. 1** Definition of humanoid's links, joints, coordinate systems

$q = [y_0, q_1, q_2, \dots, q_{17}]^T$  means the relative position between foot and ground and those of joints. Then, we have prepared 20 kinds of gait models according to the states of motion and contacting conditions of legs, and the gait transition diagram with the transition conditions is shown in Fig. 2. Based on it, we have realized bipedal walking in previous researches [9–12]. For example, the gait transition of bipedal walking is indicated by bold line arrows as 1 ? 2 ? 6 ? 10 ? 18 ? 1. Note that which pass the humanoid model transits depends on the results of dynamical motion induced. That is, the dynamical model decided the appeared transition of walking (Table 1).

### 3 Analysis of arm swing

Opposite-phase arm swing is a typical pattern seen during human’s bipedal walking. The left-arm swings forward when the right leg moves forward, and vice versa for the opposite leg and arm. This arms’ motions, though natural, is not compelled by someone and not required. For example, we can walk even while executing specific manual tasks that constrain the arms from swinging (e.g., holding an object with two hands or carrying a suitcase). However, without any particular coercion, the arm movements look following a consistent arm-swinging pattern. In this section, the causality for the generation of this



$f_{sy}$ : The force on a foot of supporting leg  
 $f_{ly}$ : The force on a foot of lifting leg  
 $f_{sf}$ : The static frictional force on a supporting leg  
 $f_{lf}$ : The static frictional force on a lifting leg  
 $y_s$ : The foot slip speed on a supporting leg  
 $y_l$ : The foot slip speed on a lifting leg  
 $\epsilon$ : 0.001[m/s]

$z_h$ : The distance from a contact surface to a heel of supporting leg  
 $f_r$ : The Normal force on a heel of supporting leg  
 $q_e$ : The angle between a contact surface and a sole centered on a heel of lifting leg  
 \*1: Supporting-foot is switched from one foot to the other foot  
 \*2: Case of walking to prevent slip  
 \*3: Case of coefficient of friction is very low and walking utilizing slip

Fig. 2 Translation of bipedal walking

natural arm motion above is analyzed qualitatively from a dynamics perspective.

The angular acceleration of the shoulders joints directly determine the movement of the arm-swing. Eq. (1) can calculate the angular acceleration of the right shoulder (joint-11, abbreviated as j-11) and left shoulder (j-14) as the following inner product [19].

$$\ddot{q}_{11} = \sum_{i=1}^{17} M_{11,i}^{-1}(\tau_i - b_i) \tag{2}$$

$$\ddot{q}_{14} = \sum_{i=1}^{17} M_{14,i}^{-1}(\tau_i - b_i) \tag{3}$$

where  $M_{li}^{-1}$  means  $l$ -th row and  $i$ -th column component of inverse matrix of mass matrix  $M(q)$ .  $\tau_i$  is input torque for  $j$ - $i$ ,  $b_i$  is  $i$ -th component of vector in summation of  $h(q, \dot{q})$ ,  $g(q)$  and  $D\dot{q}$ . How much each joint affects the left and right shoulder joints is determined by  $M_{14,i}^{-1}$ ,  $M_{11,i}^{-1}$ ,  $\tau_i$  and  $b_i$ .

Using the control framework, VLA, in previous researches [6–8], the humanoid robot walking has been realized, the transition has been shown by bold arrows in Fig. 2. As its dynamical equation is derived by the NE method, it is possible to calculate constraining internal force and torque even not generating real motion.

To explore the reasons for the occurrence of the natural arm swing, an input torque of yaw rotation (j-8) with the input torques for the shoulders (j-11 and j-14) kept to be zero. The formula is as follows where  $t_e$  means the time of the supporting leg changing.

$$\tau_8 = \begin{cases} 30 \sin(\pi(t - t_e)) & (\text{when supported by right foot}) \\ -30 \sin(\pi(t - t_e)) & (\text{when supported by left foot}) \end{cases} \tag{4}$$

Simulations were conducted with conditions of  $\tau_8$  given by Eq. (4) or  $\tau_8 = 0$ . The data will be shown in the following section.

### 4 Simulation

According to Sect. 2, gait transition that is repeated stably and represented by bold arrows in Fig. 2, has been generated by the dynamical motions made by humanoid model and VLA. The friction coefficient between the foot and the ground is set to 0.7. The torques for making the humanoid stand by VLA are given by [8], and the driving torques to make the humanoid proceed are given also by [8].

### 4.1 Simulation results

Simulations were conducted with 15[s] based on the experimental conditions that is  $\tau_i = 0$  ( $i = 8, 11, \dots, 16$ ). Figure 3 shows the screen-shot, the arms' angles and the angular accelerations of the humanoid, where a stable oscillation appears after transition response of about 5[s]. In 15 s the humanoid walked 23 steps with a distance of 11.19 metres.

Since there was no input in the shoulders and arms, Fig. 3 shows that the synchronous arm-swing occurred in the same direction with the same phase. The spiking accelerations appeared in Fig. 3c are derived from impact accelerations when the heels contacted with the ground. When there is an input torque of yaw rotation (j-8), even if the shoulders joints have no input torque, Fig.4 shows that symmetrical arm movements occurred during humanoid bipedal walking, having confirmed the causality that vibration in the yaw

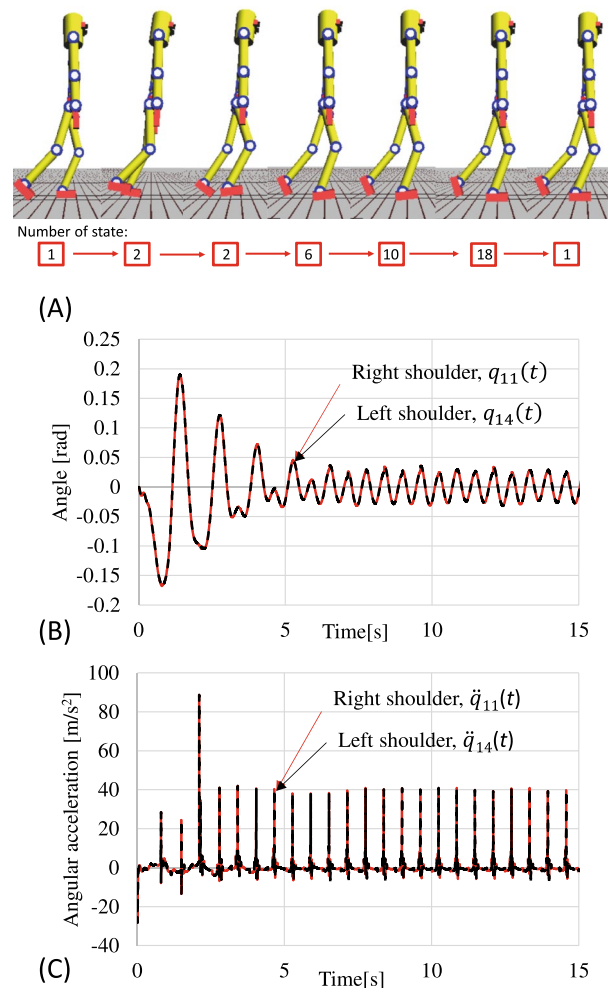
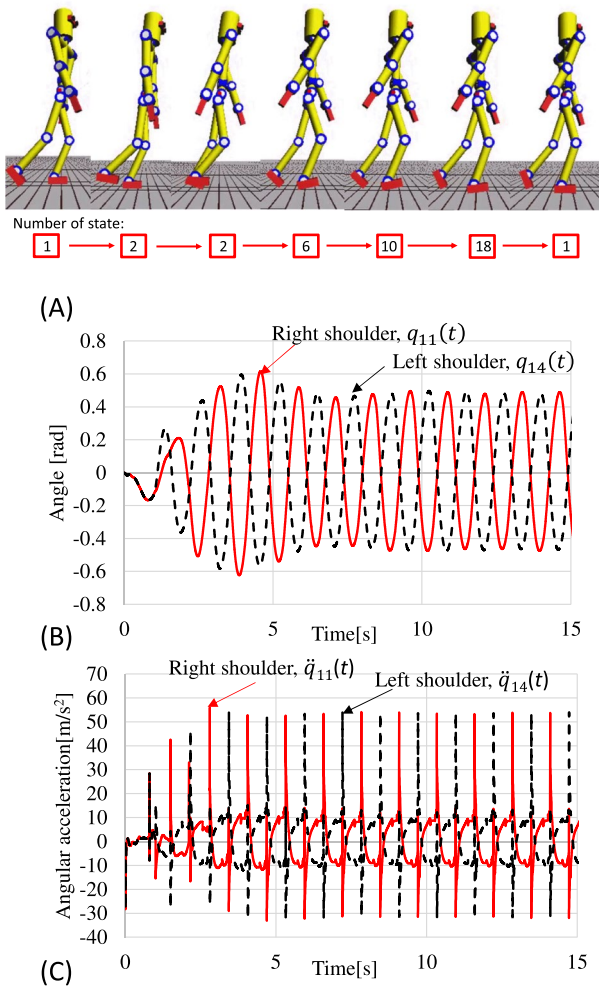


Fig. 3 With no input torque to yaw rotation,  $\tau_8 = 0$ . a is the screen-shot and the number means the gait appeared in Fig. 2, (b) is the angle of the shoulders and (c) is the angular acceleration of the shoulders



**Fig. 4** With input torque to yaw rotation,  $\tau_8$  given by Eq. (4). **a** is the screen-shot and the number means the gait appeared in Fig. 2, **(b)** is the angle of the shoulders and **(c)** is the angular acceleration of the shoulders

rotation of the torso is at least one of the reasons to cause natural arm swinging. Though it cannot be said that the yaw motion is the only reason to generate symmetrical swinging. In this case, the humanoid walked 23 steps with a distance of 11.27 m in 15 s. The insight data were analyzed by NE Method in the next subsection.

**4.2 Analyses of the data**

To make thorough inquiries into how the input torque of the yaw rotation influences the arm swing through dynamic coupling, we take out the data of the terms when calculating  $\ddot{q}_{11}$  and  $\ddot{q}_{14}$  by Eqs. (2), (3). Since the humanoid model has 18 joints, it is hard to show all of the data in this document. We divided the whole body joints into two parts to explore the insight of dynamical coupling, the lower limbs (from j-1 to j-7), the upper limbs (from j-8 to j-17).

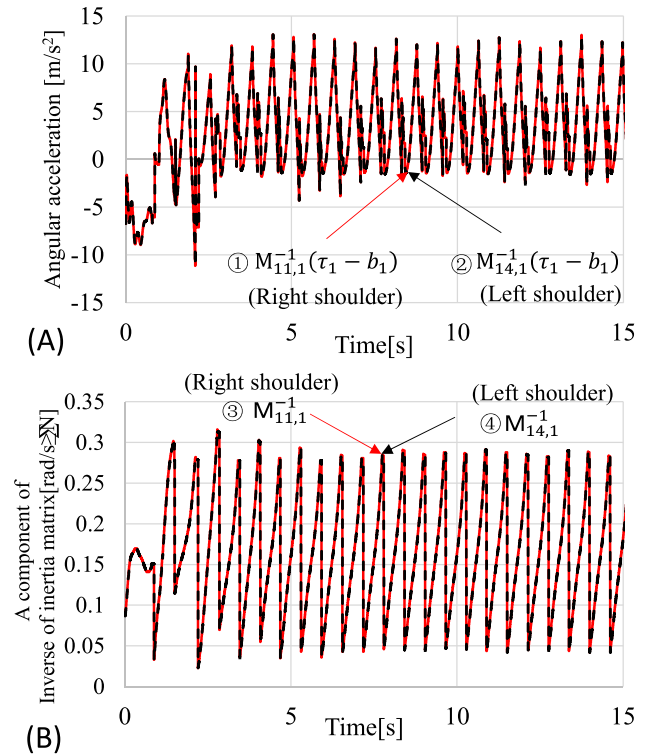


**Fig. 5** With no input torque to yaw rotation,  $\tau_8 = 0$ . **a** is the angular acceleration and **(b)** is the inverse of inertia matrix of the joint of the toe (j-1). ① means the angular acceleration made by j-1 to the right shoulder; ② means the angular acceleration made by j-1 to the left shoulder. ③ means the inverse of inertia matrix between j-1 and the right shoulder; ④ means the inverse of inertia matrix between j-1 and the left shoulder

**4.2.1 Without input torque to yaw rotation**

Firstly, considering the case of no input torque in both yaw rotation of the body (j-8) and the shoulders (j-11 and j-14), the same conditions for the walking shown by Fig. 3, the influences from j-1 to shoulders are shown in Fig. 5. It shows the angular acceleration (A) and the component of inverse of inertia matrix (B) that evaluating how the toe rotation affects the acceleration of the shoulder joints. Since the numerical value of  $M_{14,1}^{-1}$  and  $M_{11,1}^{-1}$ , one of the lower-limb portion (③ and ④) are consistent with each other, the toe rotations contribute equally to the acceleration of  $\ddot{q}_{11}$  and  $\ddot{q}_{14}$ , the left and right shoulders (① and ②).

Secondly, considering the waist, we take the joint of the yaw rotation of the body (j-8) as an example, as shown in Fig. 6. It shows that the coupling terms  $M_{14,8}^{-1}$  (from j-8 to j-14) and  $M_{11,8}^{-1}$  (from j-8 to j-11) (③ and ④) have always opposite sign. However, when there is no input in the yaw rotation,  $\tau_8 - b_8$  is almost zero since the dynamical coupling of other joints is almost zero, so the terms of the waist (① and ②) became almost same (the sign is opposite but the absolute values are very small, leading to the difference of

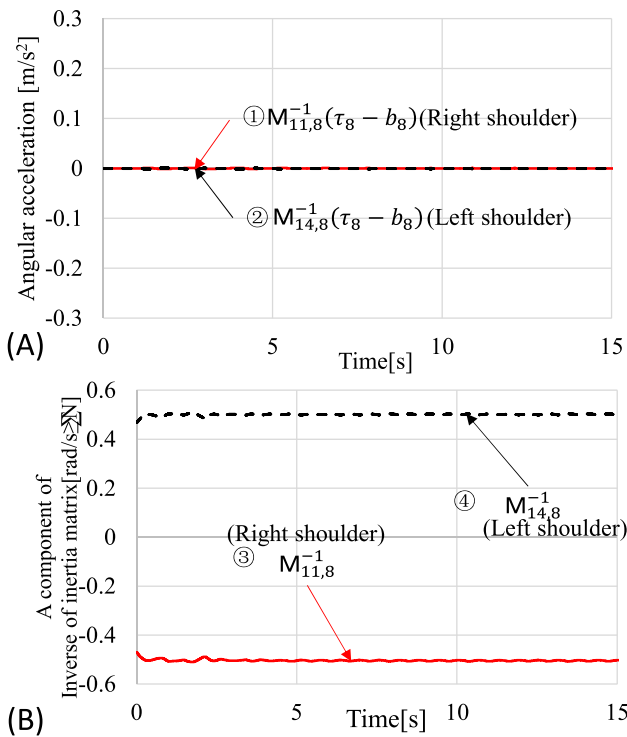


**Fig. 6** With no input torque to yaw rotation,  $\tau_8 = 0$ . **a** is the angular acceleration and **(b)** is the inverse of inertia matrix of the yaw rotation of the body (j-8)

$\ddot{q}_{11}$  and  $\ddot{q}_{14}$  being almost zero). From ① to ④, the contributions to induce opposite-phase arm-swing from j-8 to j-11 and j-14 are small, which is thought to be the reason to appear the arms' swinging to have same phase.

By summing the numerical values of the two parts, the angular acceleration of the left and right shoulder joints became equal, so synchronous arm swing appeared as shown in Fig. 3a, b.

**4.2.2 With input torque to yaw rotation**

This part considers the case that  $\tau_8$  (given by Eq. (4)) is added to the yaw rotation of the body. Firstly, we take the same joint of the toe (j-1) as an example, which is the same condition given in the previous subsection. Since the orientation of the upper limbs has inclined, the coupling from the lower limbs to shoulders ( $M_{11,1}^{-1}$  ③ and  $M_{14,1}^{-1}$  ④) changes and has a phase-shifted by  $p$  as shown by (B) in Fig. 7. The same tendency of above results appeared the shoulders accelerations indicated by ① and ② in the figure.

When calculating  $\ddot{q}_{11}$  and  $\ddot{q}_{14}$ , which include the influence from the lower limbs ( $\sum_{i=1}^7 M_{11,i}^{-1}(\tau_i - b_i)$  and  $\sum_{i=1}^7 M_{14,i}^{-1}(\tau_i - b_i)$ ) are almost the same because the model was symmetric, as shown by  $a$  and  $b$  in Fig. 8.

Then, as for the waist, we take the same joint of the yaw rotation of the body (j-8) as an example. In Fig. 9a, b, the

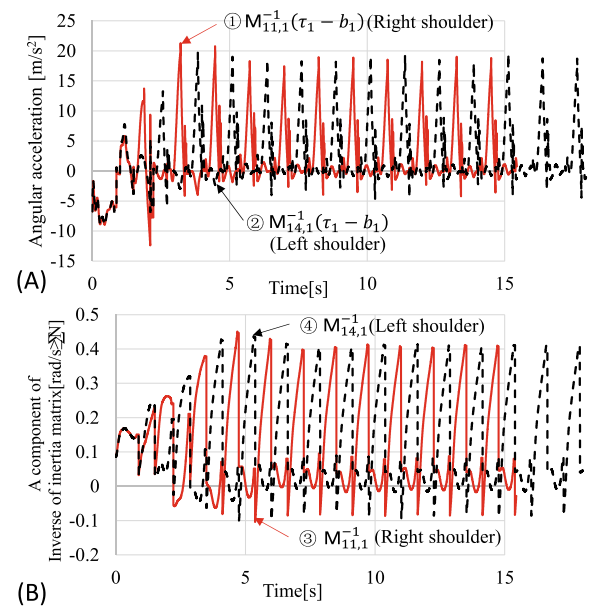


**Fig. 7** With input torque to yaw rotation,  $\tau_8$  given by Eq. (4). **a** is the angular acceleration and **(b)** is the inverse of inertia matrix of the joint of the toe (j-1)

coupling terms  $M_{14,8}^{-1}$  and  $M_{11,8}^{-1}$  (③ and ④) are almost the opposite. Then resulted the angular acceleration terms for calculating  $\ddot{q}_{11}$  and  $\ddot{q}_{14}$  have phase difference of  $p$  (① and ②).

Overall, by summing the two parts, since the angular acceleration made by the upper limbs(from j-8 to j-17) had contributed almost the opposite value in the acceleration calculation of the left and right shoulders ( $\ddot{q}_{11}$  and  $\ddot{q}_{14}$ ) as shown by  $a$  and  $b$  in Fig. 10, the symmetrical arm angle with phase difference of  $p$  appeared as shown in Fig. 4b.

According to the above data, we can conclude that when the shoulder joints have no input torque, the natural arm swing is directly related to the input torque in the yaw

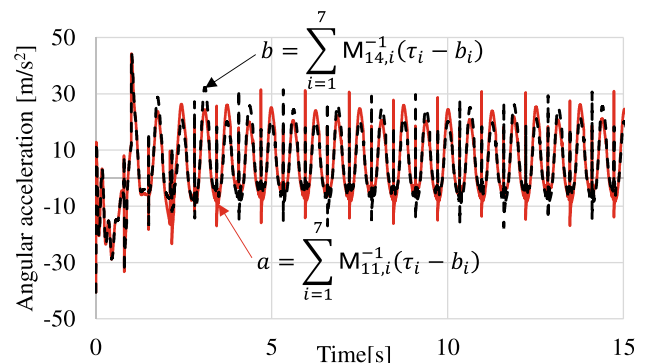


**Fig. 8** With input torque to yaw rotation,  $\tau_8$  given by Eq. (4). **a** is the acceleration made by the lower-limb to  $\ddot{q}_{14}$ ; **(b)** is the acceleration made by the lower-limb to  $\ddot{q}_{11}$

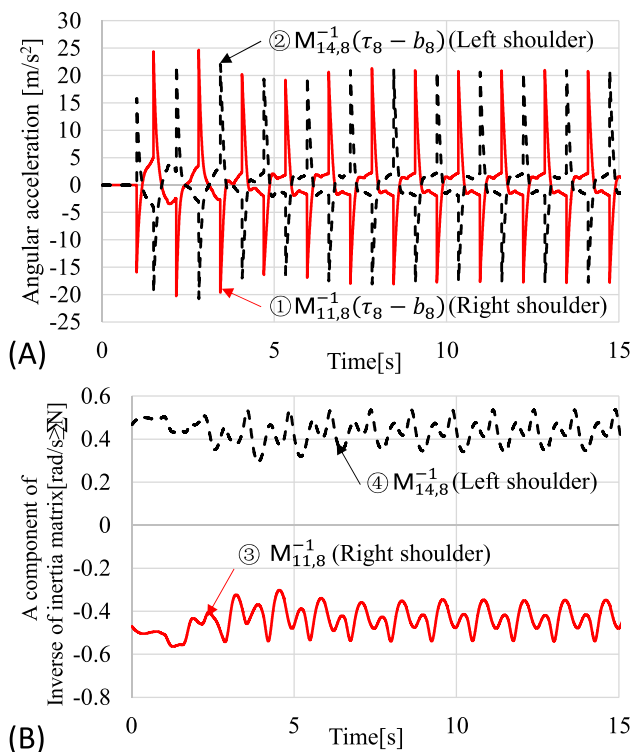


**Fig. 9** With input torque to yaw rotation,  $\tau_8$  given by Eq. (4). **a** is the angular acceleration and **(b)** is the inverse of inertia matrix of the yaw rotation of the body (j-8)

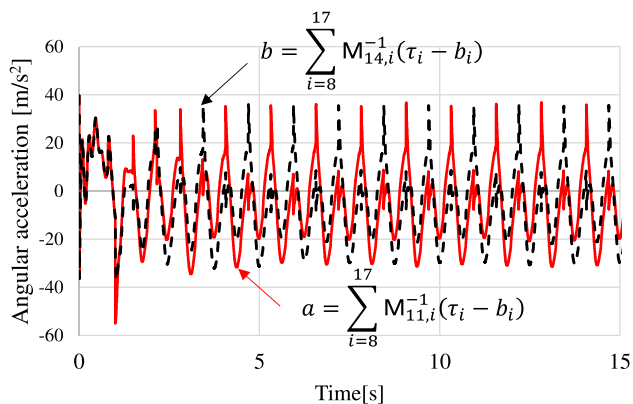


**Fig. 10** With input torque to yaw rotation,  $\tau_8$  given by Eq. (4). **a** is the acceleration made by the upper-limb to  $\dot{q}_{14}$ ; **(b)** is the acceleration made by the upper-limb to  $\dot{q}_{11}$

rotation of the body during bipedal walking. To be more specific, that the torque in the yaw rotation of the torso has different dynamic coupling on the left and right shoulder joints is one of the reason why the natural arm swing is symmetrically opposite.

### 5 Conclusion

Bipedal walkings with or without an input torque in yaw rotation of the torso have been examined when the input torque of shoulders kept to be zero. Even if the shoulder joints have no input torque, the results show that symmetrical arm movement occurred during humanoid bipedal walking. According to the results, the causality that vibration in the yaw rotation of the torso is one of the reasons to cause natural arm-swing through the dynamic coupling has been verified.

### References

- Huang Y, Chen B, Wang Q, Wei K, Wang L (2010) Energetic efficiency and stability of dynamic bipedal walking gaits with different step lengths. In: Proceedings of IEEE/RSJ international conference on intelligent robots and systems, pp 4077–4082
- Sobotka M, Buss M (2005) A hybrid mechatronic tilting robot: modeling, trajectories, and control. In: Proceedings of the 16th IFAC world congress,
- Nakamura Y, Yamane K (2000) Dynamics of kinematic chains with discontinuous changes of constraints-application to human figures that move in contact with the environments-. J RSJ 18(3):435–443
- Nishiguchi J, Minami M, Yanou A (2014) Iterative calculation method for constraint motion by extended Newton-Euler method and application for forward dynamics. Trans JSME,
- Li X, Nishiguchi J, Minami M, Takayuki M, Yanou A (2015) Iterative calculation method for constraint motion by extended Newton-Euler method and application for forward dynamics. IEEE/SICE SuE5.4,
- Song W, Minami M, Zhang Y (2012) A visual lifting approach for dynamic bipedal walking. Int J Adv Robotic Syst 9:1–8
- Song W, Minami M, Maeba T, Zhang Y, Yanou A (2011) Visual lifting stabilization of dynamic bipedal walking. In: Proceedings of 2011 IEEE-RAS international conference on humanoid robots, pp 345-351
- Li X, Minami M, Matsuno T, Izawa D (2017) Visual lifting approach for biped walking with slipping. J Robotics Mechatronics 29(3):500–508
- Feng T, Nishiguchi J, Li X, Minami M, Yanou A, Matsuno T (2015) Dynamical analyses of humanoid’s walking by using extended Newton-Euler method. AROB 20st,
- Li X, Imanishi H, Minami M, Matsuno T, Yanou A (2016) Dynamical Model of Walking Transition Considering Non-linear Friction with Floor. J Adv Comput Intell Inform 20(6):974–982
- Maeba T, Wang G, Yu F, Minami M, Yanou A (2011) Motion Representation of Walking/Slipping/Turnover for Humanoid Robot by Newton-Euler Method. SICE Annual Conference, pp 255–260
- Kobayashi Y, Minami M, Yanou A, Maeba T (2013) Dynamic reconfiguration manipulability analyses of humanoid bipedal walking. In: Proceedings of the IEEE international conference on robotics and automation (ICRA), pp 4764-4769
- Kouchi M, Mochimaru M, Iwasawa H, Mitani S (2000) Anthropometric database for Japanese population 1997–98. Japanese Industrial Standards Center, AIST, MITI

14. Maeba T, Minami M, Yanou A, Nishiguchi J (2012) Dynamical analyses of humanoid's walking by visual lifting stabilization based in event-driven state transition cooperative manipulations based on genetic algorithms using contact information IEEE/ASME international conference on advanced intelligent mechatronics Proc, pp 7-14
15. Eke-Okoro ST, Gregoric M, Larsson LE (1997) Alterations in gait resulting from deliberate changes of arm-swing amplitude and phase. *Clin Biomech* 12(7–8):516–521
16. Sjoerd M, Onno G, Peter J, Jaap H (2010) The effects of arm swing on human gait stability. *J Exp Biol* 213(Pt 23):3945–52
17. Park J (2008) Synthesis of natural arm swing motion in human bipedal walking. *J Biomech* 41(7):1417–1426
18. Li Y, Wang W, Crompton H, Gunther M (2001) Free vertical moments and transverse forces in human walking and their role in relation to arm-swing. *J Exp Biol* 204:47–58
19. Mita T, Osuka K (1989) Introduction to robot control. [M] Corona, p 81